Title

HOW DOES BLOOD-RETINAL BARRIER BREAKDOWN RELATE TO DEATH AND DISABILITY IN PEDIATRIC CEREBRAL MALARIA?

Short title

Retinal leakage in cerebral malaria

Summary

Fluorescein angiography provides evidence that in cerebral malaria severe brain swelling and death are due to fluid egress from multiple small cerebral hemorrhages. In contrast, neurological deficits in survivors are associated with vessel leak and capillary non-perfusion.

Authors

Ian J C MacCormick* (1,2,3), Valentina Barrera* (1,4), Nicholas A V Beare (1,5), Gabriela Czanner (1,6), Michael Potchen (7), Samuel Kampondeni (7,8), Robert S Heyderman (2,9), Alister G Craig (10), Malcolm E Molyneux (2,10), Macpherson Mallewa (11), Valerie A White (12), Dan Milner (13), Paul Hiscott (1), Terrie E Taylor (8,14), Karl B Seydel (8,14), Simon P Harding (1,5)

*These authors contributed equally to this work.

Affiliations

1 Department of Eye and Vision Science, Institute of Life Course and Medical Sciences, University of Liverpool, a member of Liverpool Health Partners, Liverpool, UK

2 Malawi-Liverpool-Wellcome Trust Clinical Research Programme, Queen Elizabeth Central Hospital, Blantyre, Malawi

3 Centre for Inflammation Research, University of Edinburgh, Edinburgh, UK

4 NHS Blood and Transplant, Tissue and Eye Services R&D, 14 Estuary Banks, Liverpool UK

5 St. Paul's Eye Unit, Liverpool University Hospitals Foundation Trust, Liverpool, UK

6 Department of Applied Mathematics, Liverpool John Moores University, Liverpool, UK

7 Department of Imaging Sciences, University of Rochester Medical Center, Rochester, NY, USA

8 Blantyre Malaria Project, University of Malawi College of Medicine, Blantyre, Malawi

9 Division of Infection & Immunity, University College London, London, UK

10 Liverpool School of Tropical Medicine, Pembroke Place, Liverpool, UK

11 Department of Paediatrics and Child Health, Queen Elizabeth Central Hospital, Blantyre, Malawi

12 Department of Pathology and Laboratory Medicine, University of British Columbia, Vancouver, BC, Canada

13 American Society for Clinical Pathology, Chicago, IL, USA

14 Department of Osteopathic Medical Specialties, College of Osteopathic Medicine, Michigan State University, East Lansing, USA

Corresponding author

Nicholas AV Beare, nbeare@liverpool.ac.uk

Fax: +44 (0)151 706 5905

I confirm I had full access to all the data in the study and take final responsibility for the decision to submit the manuscript for publication.

Keywords

malarial retinopathy, cerebral malaria, blood-brain barrier, blood-retina barrier, fluorescein angiography, brain swelling

Word count

Manuscript: 3488

Abstract: 200

Abstract

Background

In cerebral malaria, the retina can be used to understand disease pathogenesis. The mechanisms linking sequestration, brain swelling and death remain poorly understood. We hypothesized that retinal vascular leakage would be associated with brain swelling.

Methods

We used retinal angiography to study blood-retinal barrier integrity. We analyzed retinal leakage, histopathology, brain MRI, and associations with death and neurological disability in prospective cohorts of Malawian children with cerebral malaria.

Results

Three types of retinal leakage were seen: Large focal leak (LFL), punctate leak (PL) and vessel leak. LFL and PL were associated with death (OR 13.20, 95%CI 5.21-33.78 and 8.58, 2.56-29.08 respectively), and brain swelling ($p<0.05$). Vessel leak and macular non-perfusion were associated with neurological disability (3.71, 1.26-11.02 and 9.06, 1.79-45.90). LFL was observed as an evolving retinal hemorrhage. A core of fibrinogen and monocytes was found in 39 (93%) white-centered hemorrhages.

Conclusions

Blood-retina barrier breakdown occurs in three patterns in cerebral malaria. Associations between LFL, brain swelling, and death suggest that the rapid accumulation of cerebral hemorrhages, with accompanying fluid egress, may cause fatal brain swelling. Vessel leak from barrier dysfunction, and non-perfusion were not associated with severe brain swelling, but with neurological deficits, suggesting hypoxic injury in survivors.

Introduction

After a period of global decline in malaria, progress has stalled with approximately 230 million cases and 405,000 deaths in 2018. 90% are in sub-Saharan Africa, mainly children under 5 years [1]. *Plasmodium falciparum* causes several inter-related life-threatening syndromes in children: severe malarial anemia, metabolic acidosis, and cerebral malaria (CM). CM has a stubbornly high mortality rate of approximately 15% despite treatment in a specialist unit, [2] but this can be higher in less well-resourced settings [3]. As well as neurological sequelae at discharge, survivors can develop neurocognitive delay, epilepsy and behavioral changes [4–6].

The development of new treatments requires a better understanding of pathogenesis for insights into improved supportive care [7]. This is hampered by the difficulty of studying the brain in vivo, and in malaria-endemic regions the challenge is magnified by lack of infrastructure and imaging.

Nevertheless, an important characteristic of pediatric CM is clear: interactions between parasitized red blood cells (pRBC) and the microvascular endothelium (sequestration) evolves into severe pathology. This includes congestion and occlusion of capillaries and venules, inflammation, and dysregulation of local coagulation [8, 9]. Binding of pRBC to endothelial protein C receptor (EPCR) has been associated with severe malarial disease, brain swelling, and blood-brain barrier (BBB) breakdown [10, 11]. MRI studies have found severe brain swelling is strongly associated with death [2]. In some patients appearances are similar to posterior reversible encephalopathy syndrome, suggesting that BBB failure, combined with venous congestion, contributes to brain swelling [12]. Findings on susceptibility-weighted imaging in children with CM are consistent with venous congestion from sequestration, inflammation and autoregulatory dysfunction [13].

The resolution of MRI is poor compared to retinal biomicroscopy. The effects of sequestration on capillaries in the retina can be visualized and are specific. The presence of malarial retinopathy on funduscopy in a comatose child with *P falciparum* improves the specificity of diagnosis [14–19]. Similarities between retina and brain suggest that retinal observations could provide insight into dynamic microvascular processes occurring throughout the central nervous system (CNS), and their relationship to severe brain swelling and death [17]. The densities of pRBC sequestration in retina and brain are correlated, and more severe retinopathy cases have more cerebral vascular congestion, mature parasites and extraerythrocytic hemozoin [14]. Blood-retina barrier (BRB) function is dependent on endothelial cells and pericytes which are severely disrupted or lost in association with sequestration. Retinal fluorescein angiography (FA) utilizes intravenous fluorescein, a small, largely unbound molecule, to demonstrate retinal perfusion and also detect any BRB dysfunction. Fluorescein is an exquisitely sensitive marker of BRB breakdown through leakage.

FA has revealed funduscopic retinal vessel changes are due to intravascular filling defects and occlusion, demonstrated histologically to be due to sequestered pRBC [15]. A preliminary study also showed several patterns of BRB breakdown, or leakage, in pediatric CM [20], but associations between retinal leakage, brain swelling, and death or disability are unknown. We investigated the contribution of BBB breakdown to severe brain swelling, death, and neurodisability in CM by examining the BRB using FA. Given the extensive similarities between retina and brain in pediatric CM we hypothesized that leakage occurs proportionately in both retina and brain, and the effect of this leakage on mortality is mediated by severe brain swelling. We did not investigate FA as a prognostic predictor of outcome in CM.

Methods

Study design and participants

We performed a prospective cohort study of FA features and clinical outcomes in children with retinopathy-positive CM. The participants were part of a research program in Queen Elizabeth Central Hospital, Blantyre, Malawi, in which a subset had admission brain MRI. Ocular tissue from children who had undergone autopsy was also available.

We defined pediatric CM according to World Health Organization criteria: *P. falciparum* parasitemia, Blantyre Coma Score <3, and no other evident cause of coma [8]. This definition is broad and inevitably includes other conditions causing coma in endemic areas where asymptomatic parasitemia is common. We therefore limited our study to participants with malarial retinopathy [8,18]. An ophthalmologist performed dilated indirect ophthalmoscopy and standardized grading [21]. Retinopathy was present if one or more of these signs were seen: retinal hemorrhage, retinal whitening, orange or white vessel discoloration [22].

Clinical outcome was determined at discharge as full recovery, recovery with neurological sequelae, or death. Neurological sequelae included any new neurological deficit evident on clinical examination [6].

Parents or guardians gave written informed consent. We adhered to the Declaration of Helsinki, and the ethics committees of University of Malawi College of Medicine and Michigan State University approved the study.

Prospective retinal and brain imaging study

We recruited patients during the malaria seasons of years 2006 to 2014, excluding 2011 when FA was not performed. After clinical stabilization and dilated indirect ophthalmoscopy, patients underwent FA, and from 2009, brain MRI on the day of, or day after admission. Patients were excluded if they did not have FA within this timeframe. FA and MRIs were not performed if the child was clinically unstable, or had rapidly resolving coma.

Retinal imaging and grading

An ophthalmologist took 50º color and FA images using a table-mounted camera (Nikon D1-H; Topcon TRC-50EX; Imagenet 2000, Topcon, Japan). Sodium fluorescein 20% was injected intravenously, dosed by weight (5-10kg 2ml; 11-20kg 3ml; 21-30kg 4ml; >30kg 5ml). Images were taken over 10 minutes covering approximately a 100º field. There were no adverse reactions to fluorescein. Images were dual graded by masked observers with adjudication, in The Liverpool Ophthalmic Reading Centre according to a standardized protocol that classifies the type and severity of FA features with good inter-rater reliability [23].

Brain imaging and grading

Images were acquired using a 0.35T Signa Ovation Excite MRI scanner (General Electric, Milwaukee, USA) as reported previously [2]. Patients were comatose and not sedated. Two radiologists independently interpreted each MRI, masked to clinical outcome and retinopathy status. Differences were resolved by consensus according to pre-specified criteria [24]. Brain volume was scored according to the appearance of the cerebral hemispheres on axial T2-weighted images using a scale from one to eight. Scores of seven and eight were prespecified as life-threatening brain swelling, and involved marked sulcal effacement, without (score 7), or with evidence of uncal, subfalcine, or tonsillar

herniation (score 8) [2]. Agreement about the presence of severely increased brain volume is 87%, with kappa 0.73 (95%CI 0.61-0.83).

Retinal histopathology

Single eyes from 21 subjects with retinopathy-positive CM included in the autopsy component of the research program (1996-2010) were analyzed as described previously [14]. We scored the histopathological severity of retinopathy according to a scale of intensity of retinal sequestration and maturation of sequestered parasites [14].

After fixation in 10% v/v buffered formalin ocular specimens were opened horizontally in the pupil-optic nerve plane, or by an equatorial incision.

Gross pathology assessment was performed with a dissecting microscope, and retinopathy features photographed. All samples were dehydrated and embedded in paraffin wax before 4μm thick sections were cut with a manual rotary microtome (at least 100 sections per specimen). We investigated white-centered hemorrhages by making serial sections on 42 hemorrhages from 15 cases. Four hemorrhages were isolated by punch biopsy and embedded separately. Sequential sections were stained with hematoxylin and eosin (for staging and hemozoin), Martius-Scarlet-Blue (for fibrin), Periodic Acid-Schiff (for platelet-fibrin clots) and by immunohistochemistry to assess vessel integrity, clotting, and inflammation (Supplementary Table 1). We examined a minimum of 50 capillaries and 50 venules (diameter of 5-50μm) per case using an Olympus BX60 system microscope.

Statistical analysis

We assessed individual variables graphically and numerically and collapsed categories if less than five to ensure stable estimation. We collapsed the original brain swelling variable: combining grades 1-3, 4-6 and 7-8 (severe). We used data from one eye per patient (more severely affected for each variable) and excluded subjects with missing data. We compared eligible patients who had admission imaging with those who did not to assess selection bias (Supplementary Tables 2 and 3).

We used a multiple correspondence analysis (MCA) to explore associations between FA variables, clinical outcome, and severe brain swelling [25]. This analysis allows visualization of multivariate associations in two dimensions and does not test the statistical significance of individual associations. To do this we analyzed clinical outcome as a nominal dependent variable (with multinomial logistic regression), and brain swelling as an ordinal dependent variable (ordered logistic regression). We did a mediation analysis to clarify the relationship between retinal leak, severe brain swelling and death [26, 27].

We tested associations with histological features using ANOVA and Spearman rank correlation. We report odds ratios (OR) with 95% confidence intervals and considered the 5% level to be significant. We used Stata version 13 (Statacorp, Texas).

Results

Fluorescein Angiography

We performed FA on 260 children with CM out of 549 admissions with malarial retinopathy, and 134 also had brain MRI (Supplementary Figure 1 shows the cohort derivation). FA was completed on the day of admission in 90% and MRI in 80%. All completed imaging within 48 hours.

The group's characteristics are summarized in Supplementary Tables 2 and 3. Subjects having FA on average had worse malarial retinopathy on funduscopy, longer coma, more convulsions, lower lactate, higher LP opening pressure, and more neurological sequelae than patients who did not ($p<0.05$). Subjects who had FA and MRI had a longer median coma duration, more neurological sequelae, lower lactate, and worse malarial retinopathy than patients who had neither ($p<0.05$).

Three patterns of fluorescein leakage were identified, large focal leak (LFL), punctate leak (PL) and vessel leak (Figure 1). Vessel leak was predominantly post-capillary venule leak and larger venule leak which were analyzed separately. Vessel leak could be widespread or affecting short segments. Capillary non-perfusion (CNP), in the macula and fundus periphery, were seen in nearly all subjects (the frequencies of FA features are shown in Table 1).

Associations between FA features and outcome

An MCA of FA features, severe brain swelling and outcome shows separate clusters around recovery, death and neurological sequelae (Figure 2). Both LFL and PL cluster with death and severe brain swelling. Vessel leak and peripheral CNP cluster with neurological sequelae. These associations were controlled for all plotted variables.

The MCA findings were confirmed with regression models of clinical outcome. Multinomial logistic regression revealed unadjusted associations between death and LFL (>1 site, 13.20, 5.21-33.78) and PL (>5 sites 8.58, 2.56-29.08), ($p<0.001$ for both). Neurological sequelae were associated with post-capillary venule leak (grade 3-4, 3.71, 1.26-11.02) ($p=0.02$), and peripheral CNP (grade 3-4, 2.69, 1.07-

6.83) (p=0.04) (Table 2). Macular CNP grade 4 was associated with neurological sequelae (9.06, 1.79-45.90) (p=0.008) and death (11.52, 1.30-102.02) (p=0.03).

Associations between FA features and severe brain swelling

Ordered logistic regression of FA features and brain swelling revealed significant unadjusted associations with PL (>5 sites: 3.6, 1.2-11.1, p=0.02) and LFL (>1 site: 4.8, 1.5 to 15.5, p=0.01) (Table 3); but not with vessel leak or CNP.

Mediation analysis showed that the association between LFL and death was consistent with mediation via brain swelling rather than directly, assuming no significant confounders (p=0.02) (Supplementary Table 4). The association of PL to death was not significant as a binary variable due to smaller numbers with severe PL (>5 sites).

Pathogenesis of FA features

Serial images from six subjects demonstrated progression from LFL into a new blot or white-centered hemorrhage (Figure 3). In contrast PL did not correlate with obvious features on color images. Vessel leak was common and sometimes seen adjacent to areas of CNP, which may be reperfusing (Supplementary Figure 2). Breakdown of the BRB or vessel leak in ischemic zones is a feature of other retinal conditions such as diabetic retinopathy [28].

Histopathology

Single eyes from 21 subjects were available for histopathology, 4 of whom had FAs in life.

Retinal white-centered hemorrhages and Large Focal Leak

We analyzed sections from 15 cases with white-centered hemorrhage (42 hemorrhages) including 3 with LFL. White-centered hemorrhages typically occurred in the deep capillary plexus, and had a dense core of fibrinogen and fibrin (39/42 hemorrhages with fibrinogen (Figure 4); 28/42 with fibrin). Vessel remnants were not commonly seen, suggesting the originating vessel was small or completely disrupted. Intact pRBC were uncommon within hemorrhages, but hemozoin from ruptured parasitized erythrocytes was prominent and often internalized by phagocytes *in situ*. Platelets were relatively uncommon (CD61 positive, 12/42 hemorrhages). Leukocytes were abundant (CD45 positive, 39/42); predominantly morphological monocytes with cytoplasmic hemozoin (Supplementary Figure 3). Monocytes with hemozoin were also found in parasitized capillaries and venules without hemorrhage (median (range) 30% (16 to 64%), 50 vessels/eye from 21 eyes).

Vessel Leak

To investigate the characteristics of retinal vessel leakage, we looked for extravascular fibrinogen in relation to sequestration in all 21 cases. Extravascular fibrinogen was common in the perivascular space of retinal capillaries and venules in association with more severe retinopathy ($p<0.005$, ANOVA), and associated with density of sequestration (Spearman rho=0.56, $p<0.001$) (Supplementary Figure 3). Fibrinogen was not visible around choroidal vessels, which have little or no sequestration [14].

Punctate Leak

Only one case with PL was available at autopsy, and they also had vessel leak on FA. PL was not evident funduscopically or gross pathological examination. We were unable to determine any specific histopathological features attributable to PL.

Discussion

Sequestration, and brain swelling are considered central pathological processes in CM [2, 29]. Brain swelling can result from vasogenic edema through BBB dysfunction [13], cytotoxic edema from hypoxia [30], and also hemorrhagic breaches in the BBB. We studied the retinal circulation to infer the contribution of these mechanisms to severe brain swelling, death and neurodisability in CM. We show that BRB leakage is not homogeneous but composed of distinct types with different clinical associations. While the types can coexist, large focal leak (LFL) and punctate leak (PL) associate with severe brain swelling and death, whilst vessel leakage and capillary non-perfusion associate with gross neurological sequelae. Our findings suggest that neurological sequelae and death are discrete categories, rather than part of the same scale of severity.

LFL appears to indicate a new retinal hemorrhage. We observed the onset of LFL at sites where hemorrhages occurred over 10-minute angiograms (Figure 3). The number of retinal hemorrhages, and a large increase in retinal hemorrhages are associated with death in CM [31], and correlate with cerebral ring hemorrhages [16]. Capturing two or more hemorrhages in formation during a 10-minute angiogram with a limited field of view indicates rapid accumulation of hemorrhages and LFL sites. We propose that LFL is a manifestation of rapid hemorrhage accumulation occurring in the CNS, indicating multiple focal BBB ruptures in the brain. These results suggest that multiple cerebral ring hemorrhages are a driver of fatal brain swelling through physical breaches of the BBB. The association between LFL (hemorrhage accumulation) and death is mediated by brain swelling, giving statistical support to the biological plausibility of this hypothesis. Hemorrhages in the retina and the brain are not just signs of collateral damage to capillaries and venules, this investigation suggests they are an integral step in the development of severe brain swelling because any egress of blood cells will be accompanied by a significant fluid volume. Accumulating enough breaches in the BBB over a short time can overwhelm compensatory mechanisms and prove to be fatal.

Retinal white-centered hemorrhages have a core of fibrin(ogen) and monocytes with phagocytosed hemozoin. These are also evident in some small vessels without hemorrhage. These novel histological findings are consistent with the histopathology of cerebral ring hemorrhages [29], and presence of monocytes in brain vessels [32]. Monocytes are stimulated to release a pre-phagocytic oxidative burst by the combination of hemozoin and fibrinogen [33]. Occlusion of vessels with sequestered pRBCs alone does not cause hemorrhage [15]. Parasite binding to EPCR and consequent blockade of activated protein C (APC) may contribute to a pro-inflammatory as well as pro-thrombin state with unregulated thrombin generation and fibrin deposition [29, 34]. Hemorrhages and LFL could be related to interactions between schizont rupture, release of hemozoin and HRP2, pro-thrombogenic state and inflammatory responses from circulating monocytes. One or more of these processes result in rupture of capillary walls. Multiplied up countless times by synchronous schizont rupture, this could result in a rapid egress of fluid into the extracellular space within the cranial cavity.

Punctate leak is more difficult to characterize as it does not correspond to other FA or clinical features. We have not been able to identify a histological correlate. Even with stereoscopic images it is unclear whether it arises from retinal capillaries or the retinal pigment epithelium which constitutes an outer BRB [23]. It was seen at 1-5 sites in approximately 25% of FAs, and >5 sites in only 5%, which is the group clustering with death in the MCA. Given the widespread and visible presence of sequestration in retinal vessels it seems unlikely punctate leak is directly related to sequestration. Increased transluminal pressure could plausibly account for the appearance of PL, if sufficient to force fluorescein through the endothelium where integrity has been affected by loss of EPCR [29]. If such leakage also occurs in the brain, the association between PL and death might suggest that hydrostatic edema plays an important role in the 20% of autopsy cases without brain hemorrhage, where fibrinogen is seen around vessels

packed with pRBC [30]. Alternatively PL may indicate failure of the outer BRB, a sign of severe systemic infection and tissue dysregulation, and when widespread, a pre-agonal event.

Vessel leak occurred in nearly 50% of CM patients with retinopathy on admission, and with capillary non-perfusion (CNP) was associated with the development of neurological sequelae. In admission FAs vessel leak was often observed with CNP, and in subsequent FAs, it developed in vessels crossing, adjacent or reperfusing areas of CNP (Supplementary Figure 3). Vessel leak is indicative of vasogenic edema, presumably mediated by endothelial activation from parasite factors eg HRP2 [35] and host factors eg angiopoetin-2 [29]. In the retina it also occurs in concert with patchy tissue hypoxia and consequent cytotoxic edema. However vessel leak is associated with neurological sequelae rather than severe brain swelling and death. This association may be mediated through CNP and associated reperfusion injury, with patchy CNP in the brain leading to neurological sequelae and more subtle neurocognitive deficits which commonly develop after CM [5] (but not tested here). Diffuse axonal injury and myelin damage is seen at autopsy associated with sequestration, but not ring hemorrhages, and is likely an effect of hypoxia [30]. Vasogenic oedema from endothelial barrier disruption [29] and vessel leak is insufficient to be associated with severe brain swelling, but the associated tissue hypoxia may cause deleterious effects on brain function in survivors.

Our results introduce the concept that neurological vessel leak (vasogenic edema) and CNP (ischemia) are typical states for CM, survivable with a risk of neurological sequelae; but that severe brain swelling and death become much more likely in the face of multiple hemorrhagic breaks in the BRB/BBB represented by LFL and ring hemorrhages. Fatal brain swelling resulting from hemorrhagic leaks or physical breaches rather than diffuse disruption of endothelial tight junctions. Thus death is not on a

continuum of severity with neurological sequelae, but is rather a distinct pathological process and both may need separate mitigating interventions.

Our study has limitations. Selection bias is possible. Children with both very mild and very severe disease were less likely to tolerate retinal or brain imaging, and this is consistent with differences in retinopathy severity and coma duration in these groups. Missing mild and severe cases could lead to bias, and our results may not be generalizable to all degrees of disease severity. We present extensive descriptive data to allow comparisons with our study groups. Unmeasured confounders are possible in observational studies, although these were well-characterized clinical cases. Another limitation is the lack of comparative brain histopathology from paired cases, because autopsies discontinued after the introduction of FA.

We studied the BRB to make inferences about brain and BBB pathology. In summary, our FA data shows that leakage in the retina is not homogenous but consists of three types, which are associated with different clinical outcomes. This indicates that the events causing death versus neurological disability may be qualitatively distinct, rather than varying only by severity. Vessel leak is commonly seen in CM in relation to sequestration and the occlusion of capillaries and venules. It is associated with neurological sequelae, and we postulate this is mediated in the brain by patchy hypoxic injury, akin to the features seen in the retina. By contrast, fatal outcome is associated with LFL caused by hemorrhage formation and a physical break in the BRB. The association between LFL and death is consistent with equivalent cerebral hemorrhage causing fatal brain swelling. Hemorrhagic breaches in the BBB with fluid egress, multiplied many times in the brain by schizont rupture and local coagulopathy, may cause fatal brain swelling and death. Punctate leak is more obscure but may relate to dysfunction of the outer BRB during a terminal or pre-agonal phase. Our data suggest new treatments

for CM need to target different mechanisms to reduce mortality, and on the other hand to improve outcomes for survivors.

Funding

This work was supported by The Wellcome Trust [grant number. 092668/Z/10/Z; Malawi-Liverpool-Wellcome Trust Clinical Research Programme [core grant number 084679/Z/08/Z}, and the National Institutes of Health [grant number 5R01AI034969].

Conflict of interests

None of the authors have any conflicts of interest related to this research.

Acknowledgments

We are grateful to the patients and their guardians for taking part in the study, as well as the clinical and other staff on the pediatric research ward. We are grateful to Lucy Culshaw, Simon Biddolph, Steve Kamiza and staff involved in performing autopsies. Thank you to Cowles Chilingulo, and other MRI staff for performing MRIs. In addition to the authors, Simon Glover also performed retinal examinations and ocular imaging and we are grateful for his contribution.

Presentation

Preliminary findings were presented at the Association for Eye Research in Ophthalmology annual congress in 2017.

Corresponding author

Nicholas AV Beare, nbeare@liverpool.ac.uk

Fax: +44 (0)151 706 5905

405 # References

1. World Health Organisation. World Malaria Report 2018. WHO. 2018. Available at: http://www.who.int/malaria/publications/world-malaria-report-2018/report/en/. Accessed 10 February 2020.

2. Seydel KB, Kampondeni SD, Valim C, et al. Brain swelling and death in children with cerebral malaria. N Engl J Med **2015** ; 372(12):1126–37.

3. Reyburn H, Mbatia R, Drakeley C, et al. Association of transmission intensity and age with clinical manifestations and case fatality of severe Plasmodium falciparum malaria. JAMA **2005** ; 293(12):1461–70.

4. Birbeck GL, Molyneux ME, Kaplan PW, et al. Blantyre Malaria Project Epilepsy Study (BMPES) of neurological outcomes in retinopathy-positive paediatric cerebral malaria survivors: a prospective cohort study. Lancet Neurol **2010** ; 9(12):1173–81.

5. Langfitt JT, McDermott MP, Brim R, et al. Neurodevelopmental impairments 1 year after cerebral malaria. Pediatrics. **2019** ; 143(2):e20181026.

6. Snow RW, Craig M, Deichmann U, Marsh K. Estimating mortality, morbidity and disability due to malaria among Africa's non-pregnant population. Bull World Health Organ **1999** ; 77(8):624–40.

7. Luzolo AL, Ngoyi DM. Cerebral Malaria. Brain Res Bull. 2019 ; 145:53-58.

8. Anonymous. Severe Malaria. Trop Med Int Health **2014** ; 19(s1):7–131.

9. Kain KC, Erice C. New insights into microvascular injury to inform enhanced diagnostics and therapeutics for severe malaria. Virulence **2019** ; 10(1):1034–1046.

10. Kessler A, Dankwa S, Bernabeu M, et al. Linking EPCR-binding PfEMP1 to brain swelling in pediatric cerebral malaria. Cell Host Microbe **2017** ; 22(5):601-614.e5.

11. Moxon CA, Wassmer SC, Milner DA, et al. Loss of endothelial protein C receptors links coagulation and inflammation to parasite sequestration in cerebral malaria in African children. Blood **2013** ; 122(5):842–51.

12. Mohanty S, Benjamin LA, Majhi M, et al. Magnetic resonance imaging of cerebral malaria patients reveals distinct pathogenetic processes in different parts of the brain. mSphere **2017** Jun7;2(3):e00193-17

13. Potchen MJ, Kampondeni SD, Seydel KB, et al. 1.5 tesla magnetic resonance imaging to investigate potential etiologies of brain swelling in pediatric cerebral malaria. Am J Trop Med Hyg **2018** ; 98(2):497–504.

14. Barrera V, Hiscott PS, Craig AG, et al. Severity of retinopathy parallels the degree of parasite sequestration in the eyes and brains of Malawian children with fatal cerebral malaria. J Infect Dis **2015** ; 211(12):1977–86.

15. Barrera V, MacCormick IJC, Czanner G, et al. Neurovascular sequestration in paediatric P. falciparum malaria is visible clinically in the retina. eLife **2018** Mar 26;7:e32208.

16. Greiner J, Dorovini-Zis K, Taylor TE, et al. Correlation of hemorrhage, axonal damage, and blood-tissue barrier disruption in brain and retina of Malawian children with fatal cerebral malaria. Front Cell Infect Microbiol **2015** ; Mar 16; 5:18.

17. MacCormick IJC, Beare NAV, Taylor TE, et al. Cerebral malaria in children: using the retina to study the brain. Brain **2014** ; 137(8):2119–42.

18. Taylor TE, Fu WJ, Carr RA, et al. Differentiating the pathologies of cerebral malaria by postmortem parasite counts. Nat Med **2004** ; 10(2):143–5.

19. Essuman VA, Ntim-Amponsah CT, Astrup BS, et al. Retinopathy in severe malaria in Ghanaian children--overlap between fundus changes in cerebral and non-cerebral malaria. Malaria Journal **2010** ; 12(9):232.

20. Beare NAV, Harding SP, Taylor TE, Lewallen S, Molyneux ME. Perfusion abnormalities in children with cerebral malaria and malarial retinopathy. J Infect Dis. **2009** ; 199(2):263–71.

21. Beare NA, Southern C, Lochhead J, Molyneux ME, Lewallen S, Harding SP. Inter-observer concordance in grading retinopathy in cerebral malaria. Ann Trop Med Parasitol. **2002** ; 96(1):105–8.

22. Lewallen S, Harding SP, Ajewole J, et al. A review of the spectrum of clinical ocular fundus findings in P. falciparum malaria in African children with a proposed classification and grading system. Trans R Soc Trop Med Hyg **1999 ;** 93(6):619–22.

23. MacCormick IJC, Maude RJ, Beare NAV, et al. Grading fluorescein angiograms in malarial retinopathy. Malaria Journal **2015** Dec ; 14(1):367.

24. Potchen MJ, Kampondeni SD, Ibrahim K, et al. NeuroInterp: a method for facilitating neuroimaging research on cerebral malaria. Neurology **2013** ; 81(6):585–8.

25. Le Roux B, Rouanet H, SAGE Publications. Multiple Correspondence Analysis. Available at: http://methods.sagepub.com/book/multiple-correspondence-analysis. Accessed 15 Aug 2019.

26. VanderWeele T, Oxford University Press. Explanation in Causal Inference: Methods for Mediation and Interaction 2015. Available at: http://ebookcentral.proquest.com/lib/ed/detail.action?docID=1920742. Accessed 3 Jan 2019.

27. Greenland S, Pearl J, Robins JM. Causal diagrams for epidemiological research. Epidemiology **1999** ; 10(1):37-48

28. Dithmar S, Holz FG. Fluorescein angiography in ophthalmology. Springer-Verlag, Berlin Heidelberg, 2008.

29. Bernabeu M, Smith JD. EPCR and Malaria Severity: The center of a perfect storm. Trends Parasitol **2017** ; 33(4):295–308.

30. Dorovini-Zis K, Schmidt K, Huynh H, et al. The neuropathology of fatal cerebral malaria in Malawian children. Am J Pathol **2011** ; 178(5):2146–58.

31. Beare NAV, Southern C, Chalira C, Taylor TE, Molyneux ME, Harding SP. Prognostic significance and course of retinopathy in children with severe malaria. Arch Ophthalmol **2004** ; 122:1141-1147.

32. Hochman SE, Madaline TF, Wassmer SC, et al. Fatal pediatric cerebral malaria is associated with intravascular monocytes and platelets that are increased with HIV coinfection. MBio **2015** Sep 22 ; 6(5):e01390-01315.

33. Barrera V, Skorokhod OA, Baci D, Gremo G, Arese P, Schwarzer E. Host fibrinogen stably bound to hemozoin rapidly activates monocytes via TLR-4 and CD11b/CD18-integrin: a new paradigm of hemozoin action. Blood **2011** ; 117(21):5674–82.

34. O'Sullivan JM, Preston RJ, O'Regan N, O'Donnell JS Emerging roles for hemostatic dysfunction in malaria pathogenesis. Blood **2016** ; 127(19):2281-8.

35. Pal P, Daniels BP, Oskman A, Diamond MS, Klein RS, Goldberg DE. Plasmodium falciparum histidine-rich protein II compromises brain endothelial barriers and may promote cerebral malaria pathogenesis. mBio. **2016** ; 7;7(3).

Table 1. Frequency of fluorescein angiogram signs, brain swelling on MRI and clinical outcomes.

CNP capillary non-perfusion, IVFD intravascular filling defect. Missing data are due to ungradable images.

Variable		Subjects with admission FA and MRI n=134 recruited 2009 to 2014		Subjects with admission FA n=260 recruited 2006 to 2014	
		%	number	%	number
Macular CNP	Grade 0 or 1	6.87	131	12.16	255
	Grade 2	47.33		45.9	
	Grade 3 or 4	45.80		41.96	
Peripheral CNP	Grade 0 or 1	39.85	133	42.8	259
	Grade 2	24.81		24.32	
	Grade 3 or 4	35.34		32.8	
Punctate leak	None	63.43	134	67.7	260
	1-5 sites	28.36		26.9	
	>5 sites	8.21		5.1	
Large focal leak	None	83.58	134	81.9	260
	1 site	6.72		8.1	
	>1 site	9.70		10.0	
	None	56.39	133	56.59	258

Larger Venule leak	Grade 1	32.33		28.68	
	Grade 2 or 3	11.28		14.73	
Post-capillary venule leak	None or grade 1	75.19	133	70.8	257
	Grade 2	17.29		19.84	
	Grade 3 or 4	7.52		9.3	
Optic disc leak	Absent	18.66	134	13.85	260
	Present	81.34		86.15	
IVFD in large arterioles	Absent	86.15	130	84.74	249
	Present	13.85		15.26	
Clinical outcome	Full recovery	73.9	134	74.6	260
	Sequelae	11.9		11.9	
	Death	14.2		13.5	
Brain swelling	Grade 1-3	13.5	133	n/a	
	Grade 4	28.6		n/a	
	Grade 5	20.3		n/a	
	Grade 6	21.8		n/a	
	Grade 7 or 8	15.8		n/a	

410

Table 2. Unadjusted associations between retinal angiographic features and outcomes (recovery with neurological sequelae, or death) with reference to subjects who recovered fully.

Associations were estimated using multinomial logistic regression, in 260 subjects with admission fluorescein angiogram. The reference category is absence of a feature (except capillary leak, macular capillary non-perfusion, and peripheral capillary non-perfusion where grades 0 and 1 were combined due to small numbers without these features). The odds ratio estimate is equal to exponential of the Coefficient. P<=0.05 are in bold.

FA feature	Outcome	FA grade	Odds Ratio	P	95% confidence interval	N
Punctate leak	Sequelae	1-5 sites	0.55	0.25	0.2 to 1.52	260
		>5 sites	0.00	0.98	0.00 to >1000	
	Death	1-5 sites	4.06	**<0.001**	1.82 to 9.12	
		>5 sites	8.58	**<0.001**	2.56 to 29.08	
Large focal leak	Sequelae	1 site	1.62	0.42	0.50 to 5.21	260
		>1 site	0.64	0.68	0.08 to 5.26	
	Death	1 site	0.55	0.58	0.07 to 4.39	
		>1 site	13.20	**<0.001**	5.21 to 33.78	
Post-capillary venule leak	Sequelae	Grade 2	1.70	0.26	0.67 to 4.26	257
		Grade 3-4	3.71	**0.02**	1.26 to 11.02	
	Death	Grade 2	0.25	0.07	0.06 to 1.11	
		Grade 3-4	1.48	0.52	0.45 to 4.81	
Larger venule leak	Sequelae	Grade 1	1.86	0.16	0.78 to 4.39	258
		Grade 2-3	2.51	0.08	0.90 to 6.89	
	Death	Grade 1	1.28	0.56	0.55 to 3.00	
		Grade 2-3	1.63	0.35	0.59 to 4.57	
Macular capillary non-perfusion	Sequelae	Grade 2	1.59	0.56	0.33 to 7.59	255
		Grade 3	1.92	0.43	0.37 to 9.88	
		Grade 4	9.06	**0.008**	1.79 to 45.90	
	Death	Grade 2	2.60	0.38	0.32 to 21.39	

		Grade 3	7.69	0.06	0.96 to 61.55	
		Grade 4	11.52	**0.03**	1.30 to 102.02	
Peripheral capillary non-perfusion	Sequelae	Grade 2	2.32	0.10	0.84 to 6.44	259
		Grade 3-4	2.69	**0.04**	1.07 to 6.83	
	Death	Grade 2	1.72	0.24	0.69 to 4.29	
		Grade 3-4	1.54	0.33	0.65 to 3.66	

Table 3. Unadjusted associations between angiography features and brain swelling. The sample is 134 subjects with both admission fluorescein angiogram and MRI brain. Associations were estimated using ordered logistic regression, P<0.05 in bold.

FA feature	FA grade	Odds ratio	p	95% CI	n
Punctate leak	1-5 sites	0.78	0.47	0.39 to 1.54	133
	>5 sites	3.62	**0.02**	1.19 to 11.09	
Large focal leak	1 site	0.47	0.25	0.13 to 1.69	133
	>1 site	4.77	**0.01**	1.47 to 15.46	
Post-capillary venule leak	Grade 2	0.76	0.50	0.35 to 1.68	132
	Grade 3-4	2.94	0.09	0.83 to 10.36	
Larger venule leak	Grade 1	1.09	0.80	0.56 to 2.15	132
	Grade 2-3	1.85	0.24	0.67 to 5.14	
Macular capillary non-perfusion	Grade 2	0.84	0.79	0.22 to 3.01	130
	Grade 3	1.97	0.32	0.52 to 7.41	
	Grade 4	1.94	0.36	0.47 to 7.98	
Peripheral capillary non-perfusion	Grade 1	3.06	0.47	0.15 to 63.30	132
	Grade 2	3.07	0.47	0.14 to 64.70	
	Grade 3	2.67	0.53	0.12 to 58.27	
	Grade 4	2.97	0.49	0.14 to 63.67	

Figure 1. Retinal leakage and severe brain swelling seen in pediatric cerebral malaria

A) Fluorescein angiographic image showing multiple Large Focal Leaks (LFL). A LFL is a large leak of fluorescein from a vessel within the retina. Note associated black masking from recent multiple blot retinal hemorrhages. Clusters of more established hemorrhages round the vascular arcades show a white central dot of the fibrin core. The optic disc has abnormal fluorescein leakage from disc swelling (papilloedema). B) Fluorescein angiographic image showing many Punctate Leaks (PL). A PL is a small fluorescein leak from deep retina or underlying retinal pigment epithelium. C) Fluorescein angiographic image showing widespread leakage from larger venules and post-capillary venules (Vessel Leak). D) Sagittal MRI of the brain showing severe brain swelling in a child with retinopathy positive cerebral malaria, with herniation of the cerebellum at the foramen magnum (arrow).

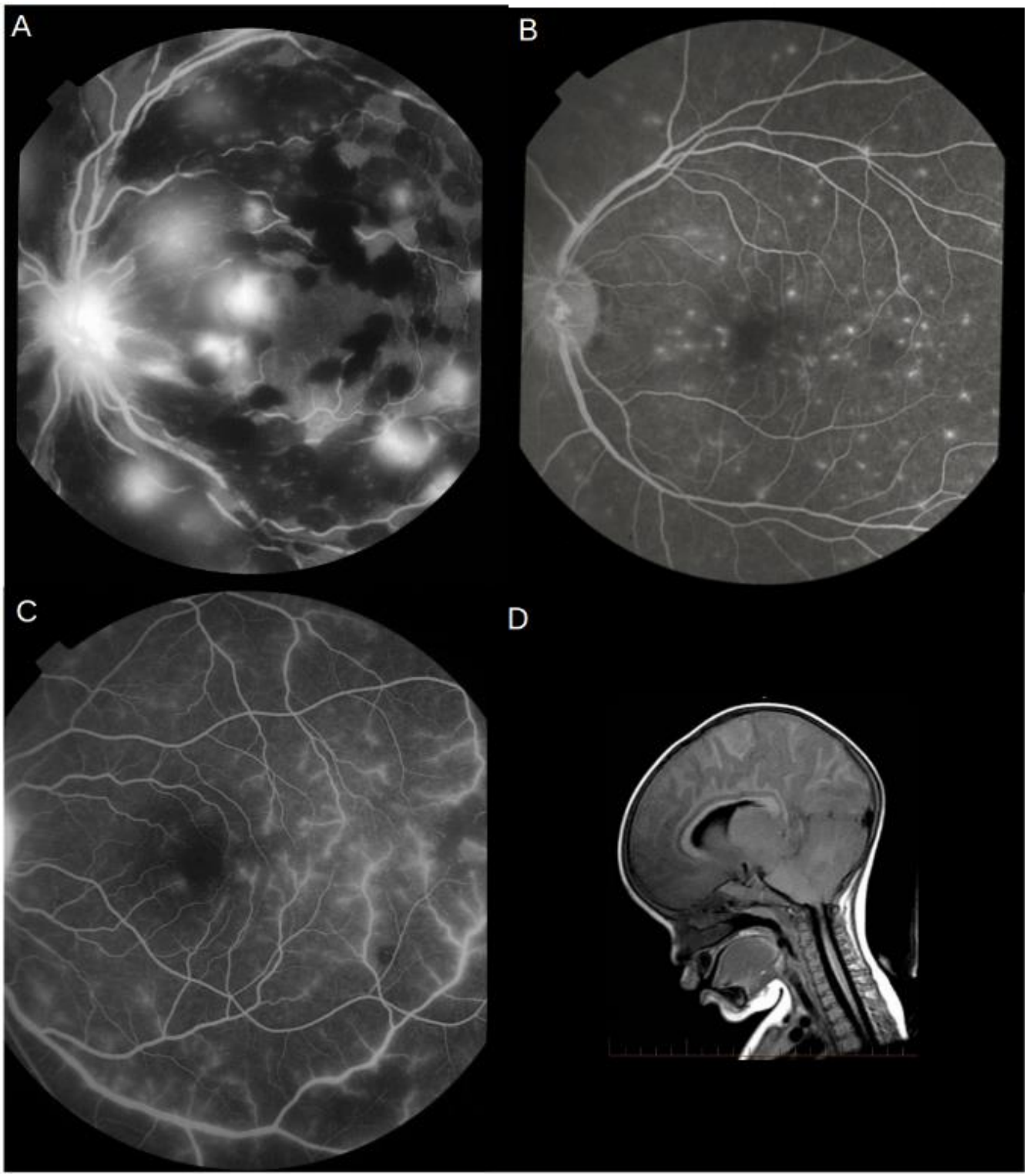
A
B
C
D

Figure 2. Multiple correspondence analysis plot showing fluorescein angiogram features cluster with different outcomes in children with cerebral malaria.

This analysis looks for multiple associations in two dimensions, and the boxes are illustrative. The severe grade of large focal leak (2), punctate leak(2), presence of arteriolar IVDF (1), and severe brain swelling (grades 7-8), cluster with death. More severe grades of larger venule (2) and post-capillary venule (2-3) leak and CNP in the retinal periphery (3) cluster with neurological sequelae. Absent or mild angiographic features cluster with full recovery on discharge. Disc Leak and Large venule IVFD, which were plotted close to the origin, have been omitted from the plot for clarity. Zero indicates the absence of a feature and ascending numbers indicate worsening severity. CNP capillary non-perfusion; IVFD intravascular filling defects.

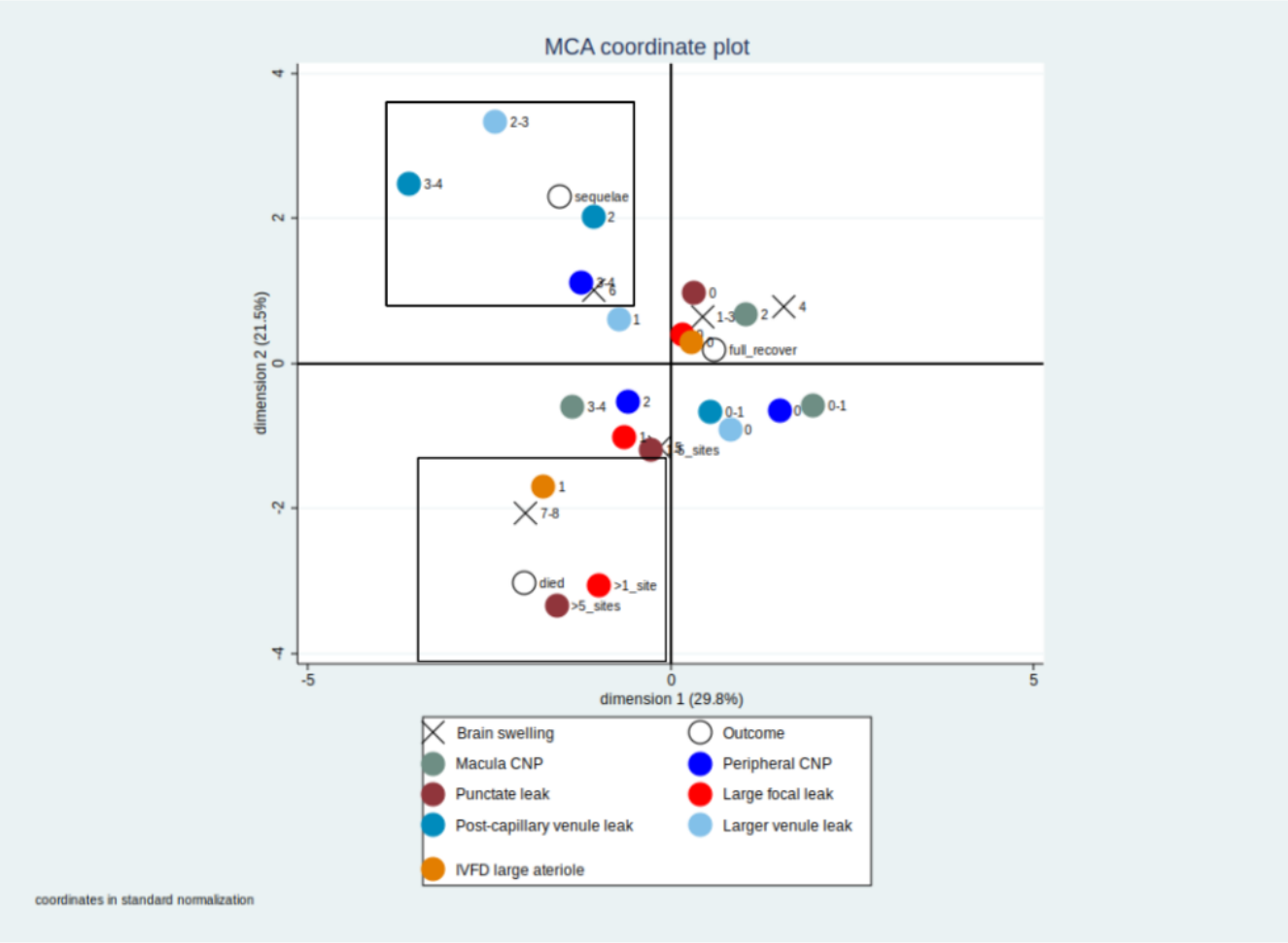

Figure 3. Development of large focal leak and co-located retinal hemorrhage during angiogram. From left to right: A) Pre-angiogram color image. B) Fluorescein angiogram at six minutes. C) Fluorescein angiogram at nine minutes: large focal leak has developed. D) Color image immediately post-angiogram shows a hemorrhage at the same site, with a halo of fluorescein.

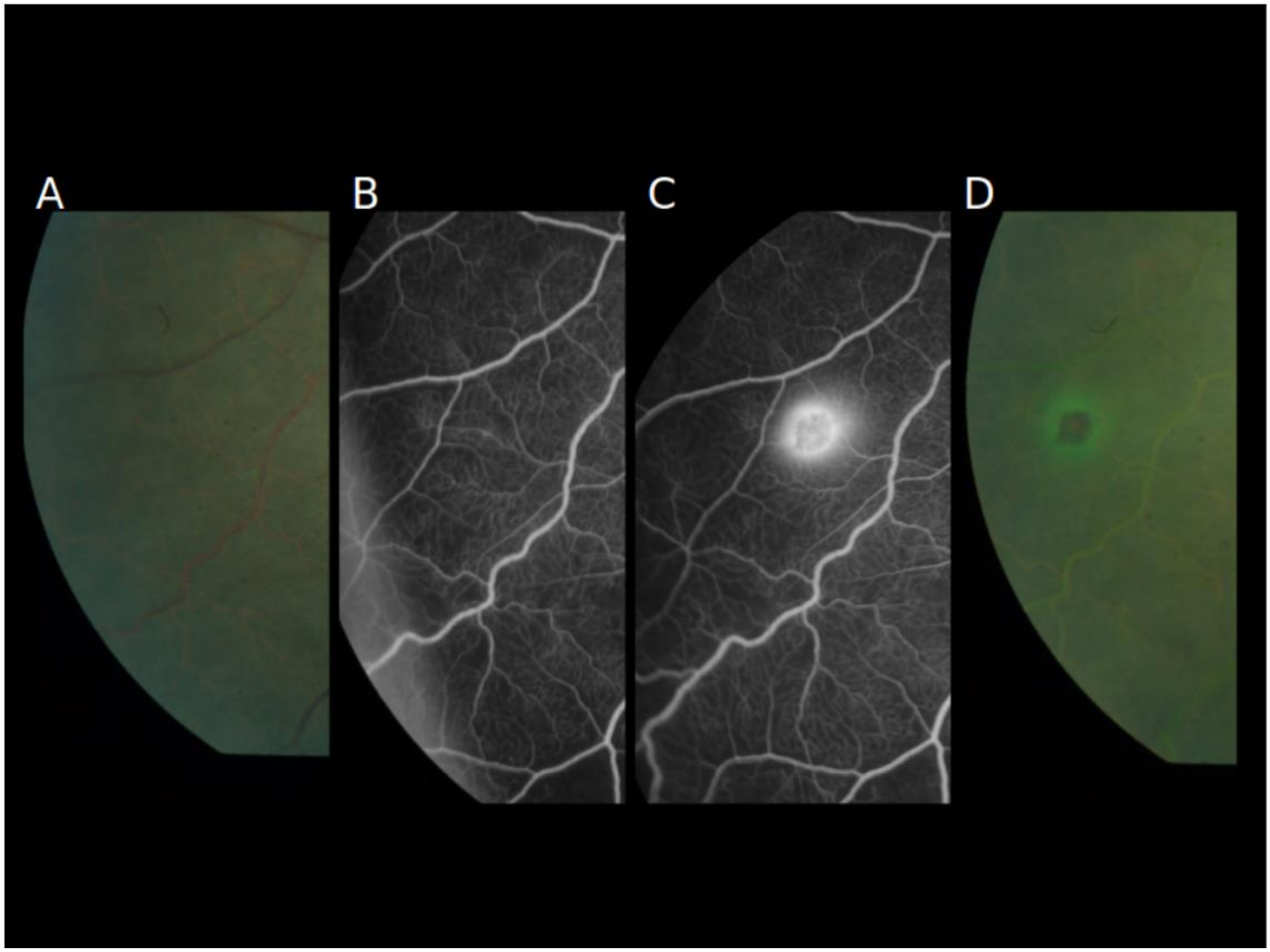

460

Figure 4. Histopathology of vascular leakage and white-centered hemorrhages.

A. Fibrinogen around a heavily parasitized microvessel (arrow), shown in red by immunohistochemistry, with blue hematoxylin counterstaining. Scale bar = 100µm. B. Gross pathology of a superior calotte used to directly sample white-centered hemorrhages in a case with moderate to severe malarial retinopathy. C. White-centered hemorrhage has a core of fibrinogen (immunohistochemistry). Scale bar = 100µm. D. Fibrinogen confirmed by hematoxylin and eosin. Hemozoin is visible as dark brown dots (arrows). Scale bar = 50µm.

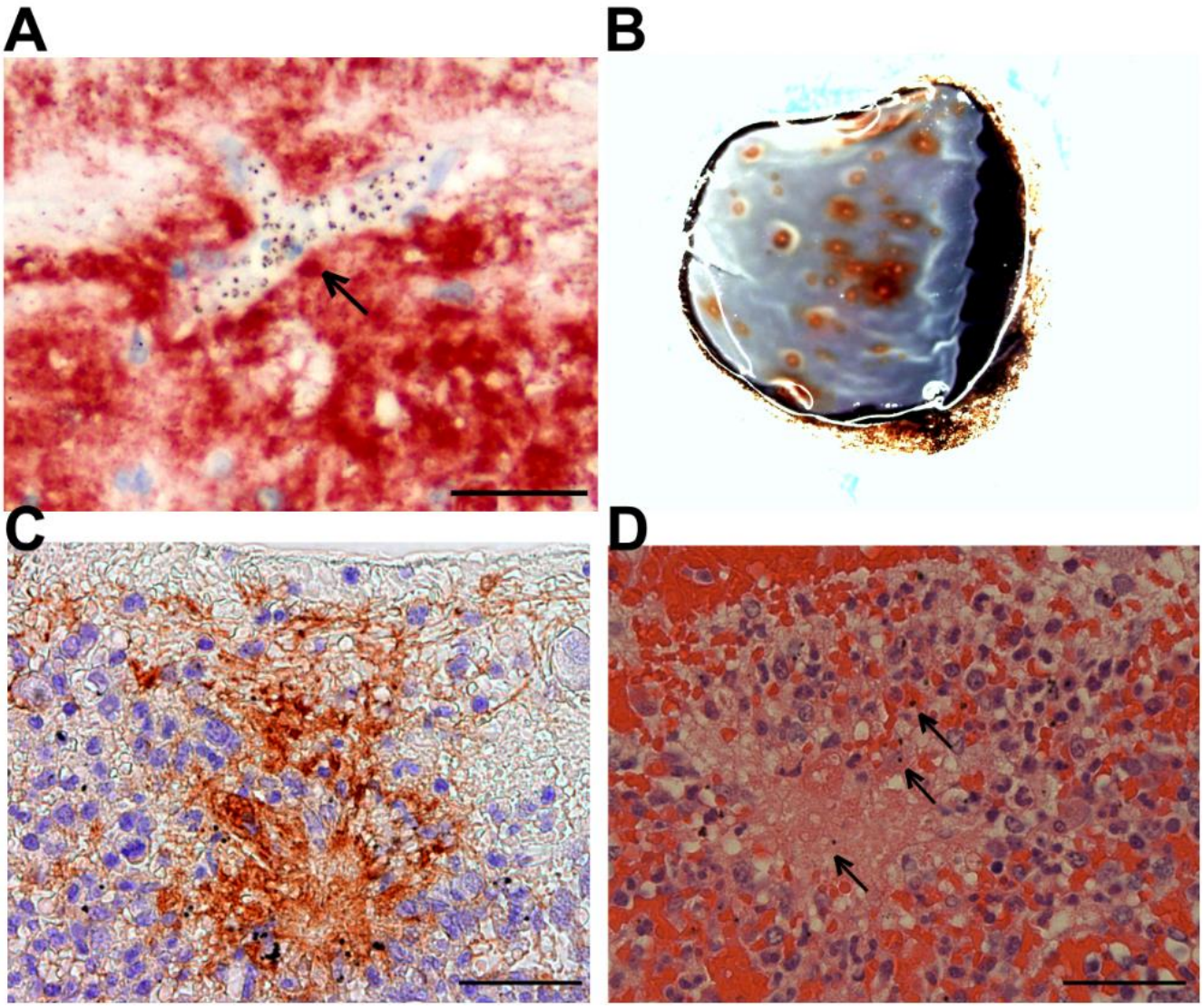

Supplementary Figure 1. Derivation of cohorts.

A) Entire fluorescein angiogram cohort. B) Fluorescein angiogram and MRI brain subset cohort. Ret- malarial retinopathy absent; Ret+ malarial retinopathy present

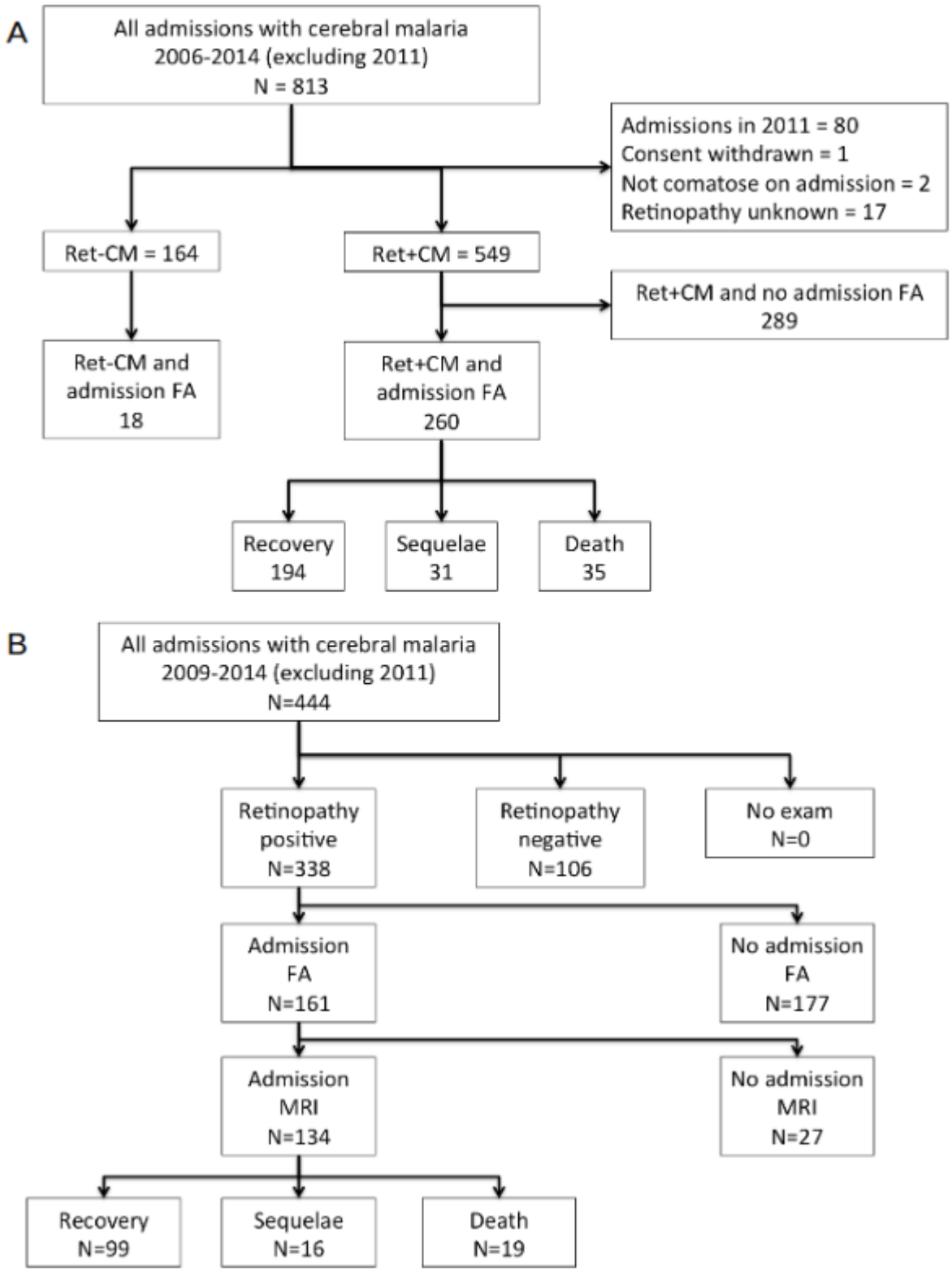
A
All admissions with cerebral malaria
2006-2014 (excluding 2011)
N = 813
Admissions in 2011 = 80
Consent withdrawn = 1
Not comatose on admission = 2
Retinopathy unknown = 17
Ret-CM = 164
Ret+CM = 549
Ret+CM and no admission FA
289
Ret-CM and
admission FA
18
Ret+CM and
admission FA
260
Recovery
194
Sequelae
31
Death
35
B
All admissions with cerebral malaria
2009-2014 (excluding 2011)
N=444
Retinopathy
positive
N=338
Retinopathy
negative
N=106
No exam
N=0
Admission
FA
N=161
No admission
FA
N=177
Admission
MRI
N=134
No admission
MRI
N=27
Recovery
N=99
Sequelae
N=16
Death
N=19

475

Supplementary Figure 2. Capillary non-perfusion and leakage

A) Admission color and fluorescein angiogram (FA) images with retinal whitening and peripheral capillary non-perfusion (CNP) and no leakage. Note the attenuated venule in center is orange, with intravascular filling defects on FA. B) Day 1 showing development of larger zones of CNP and fluorescein leakage from vessels crossing or adjacent to non-perfused zones. C) Day 2 showing improvement of CNP (re-perfusion) and leakage from re-perfusing vessels.

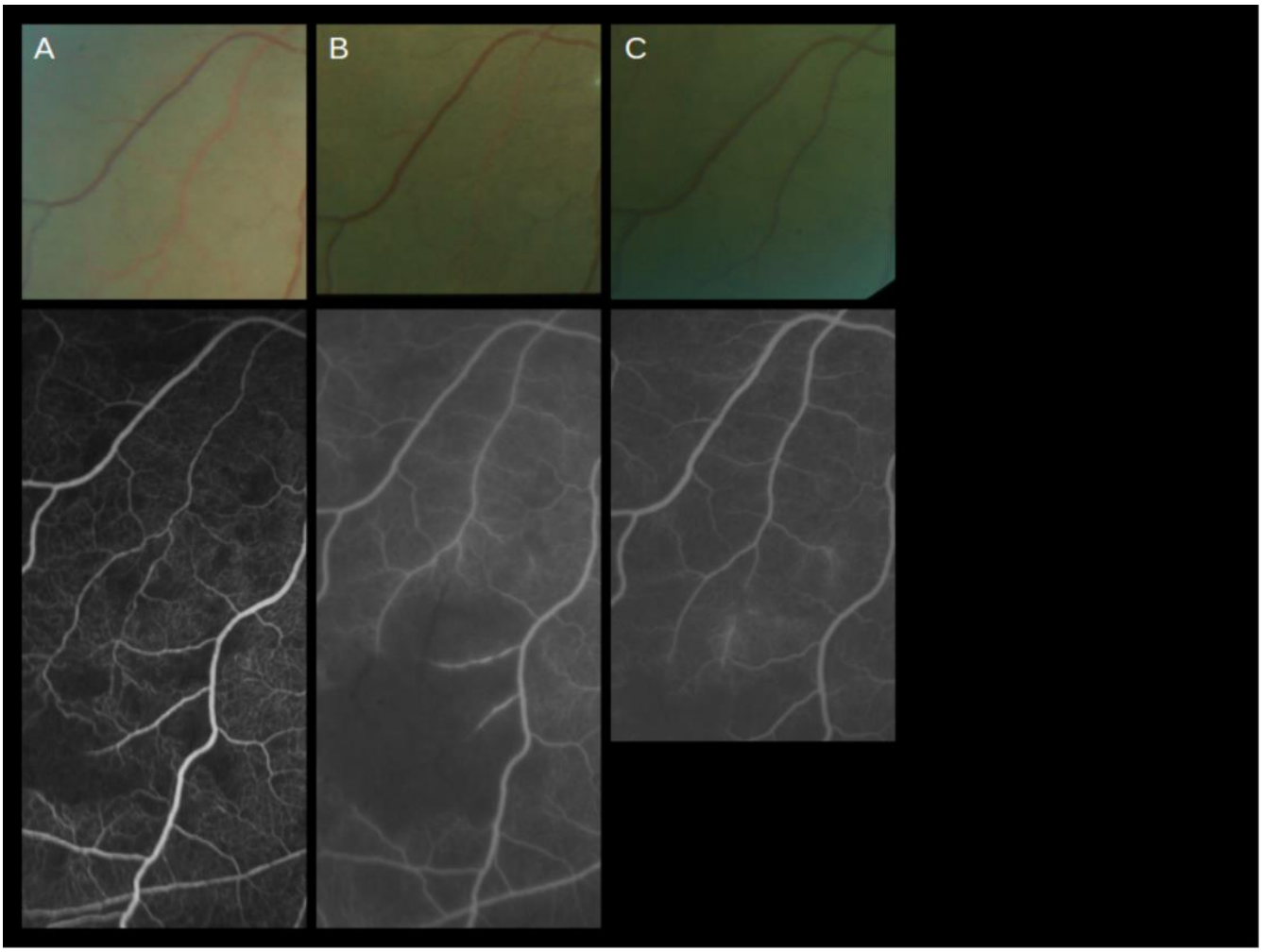

Supplementary Figure 3. Histopathology of monocytes and hemozoin.

A) Hemozoin-laden monocytes identified in the core of white-centered hemorrhages by the presence of dark brown malaria pigment and typical kidney-shaped nuclei. Cells are marked by arrows. Anti-CD45 immunohistochemistry (red) and hematoxylin (blue) counterstaining are shown. Scale bar = 20 µm. B-D) Characterization of monocytes and hemozoin by hematoxylin and eosin staining. B) Monocytes with phagocytosed hemozoin in capillaries. Scale bar = 10 µm. C) Monocytes in venules. Scale bar = 20 µm. D) Extra-erythrocytic hemozoin in retinal capillaries. Scale bar = 10 µm.

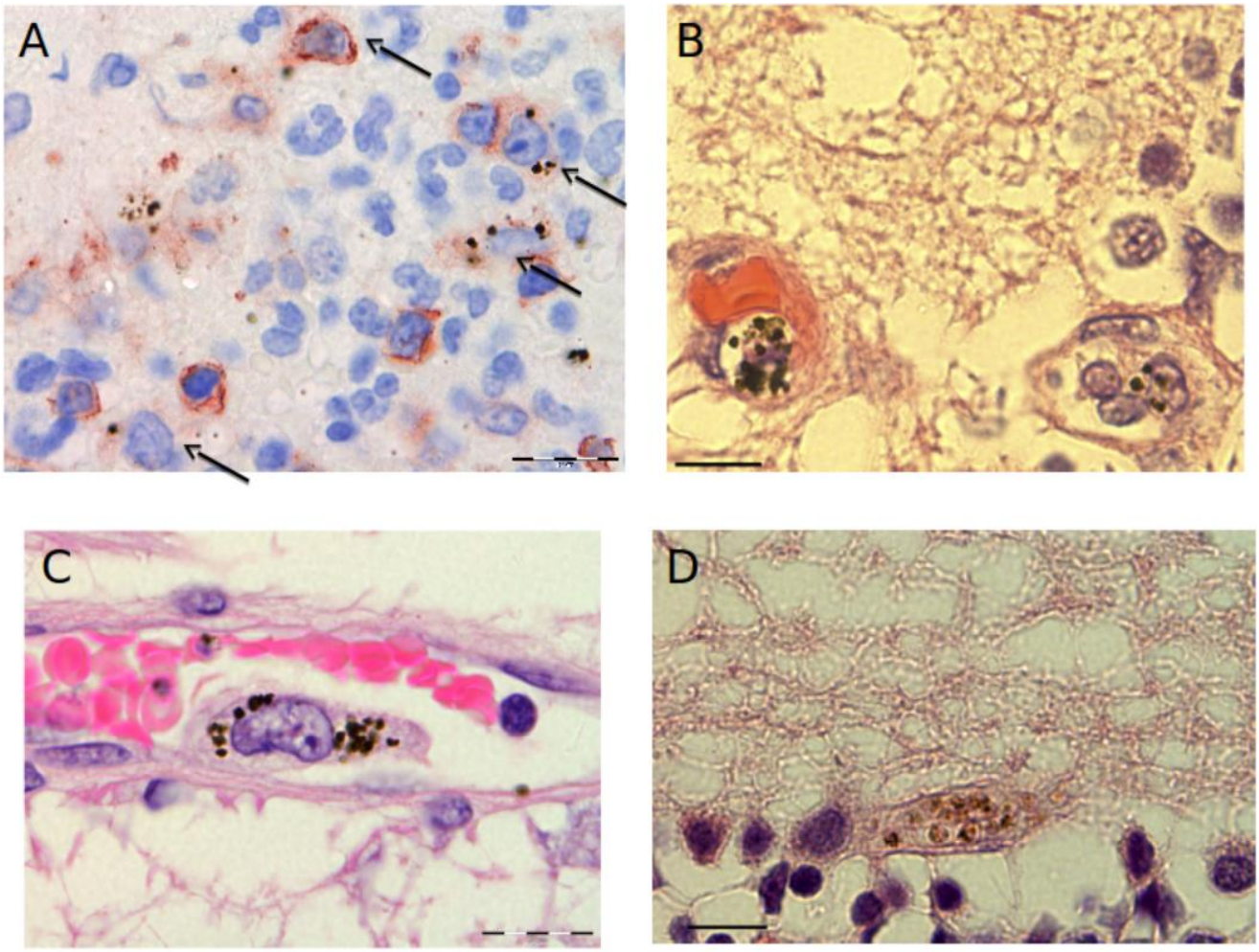

Supplementary Table 1. Antigens used to characterize features of retinal leakage.

Antigen	**Specificity**	**Feature**	**Manufacturer (clone)**	**Host* (class)**	**Ag retrieval †**	**Dilution ‡**	**Chromogen §**
CD34 (II)	Endothelium	Vessel integrity	Dako (QBEnd-10)	Ms mAb (IgG1k)	Heat (High pH)	1:100, 30 min RT	DAB
Smooth muscle actin (SMA)	Pericyte	Vessel integrity	Dako (1A4)	Ms mAb (IgG2ak)	Heat (Low pH)	1:2,000, o.n. 4°C	AEC
Laminin	Basal membrane	Vessel integrity	Sigma	Rb pAb	Proteinase K	1:500, o.n. 4°C	AEC
Collagen IV	Basal membrane	Vessel integrity	Sigma (COL-94)	Ms mAb (IgG1)	Proteinase K	1:2,000, o.n. 4°C	AEC
Fibrinogen	Plasma protein	Vessel integrity	Dako	Rb pAb	Proteinase K	1:500, 30 min RT	AEC
Fibrin	Fibrin polymer	Clotting	102-10 (gift from Dr Y Matsumura)	mAb-HRP conjugated	Heat (Low pH)	1:100, o.n. 4°C	DAB
CD61	Platelets and precursors	Clotting	Thermo Scientific	Ms mAb (IgG1)	Heat (High pH)	1:100, 32 min RT	DAB or AEC
CD45	Pan-leukocyte	Inflammation	Dako (2B11+PD7/26)	Ms mAb (IgG1k)	Heat (Low pH)	1:200, o.n. 4°C	AEC
CD68	Differentiated macrophages	Inflammation	Dako (PG-M1)	Ms mAb (IgG3k)	Heat (Low pH)	1:100, o.n. 4°C	AEC

Host: Rb=rabbit; Ms=mouse; mAb=monoclonal antibody; pAb=polyclonal antibody. † Ag retrieval: heat-mediated antigen retrieval was performed in high pH solution (10mM Tris/1mM EDTA, pH 9.0) or low pH solution (trisodium citrate 10mM, pH 6.0). Proteinase K was from Dako (ready-to-use solution). ‡ Dilution and incubation time: RT=room temperature; o.n.=overnight. § Chromogen: AEC: 3-amino-9-ethylcarbazole; DAB=3,3'-diaminobenzidine.

Supplementary Table 2. Characteristics of eligible subjects comparing those not included (without admission FA) to those included (with admission FA) in the study. Retinal data are from the worst affected eye. All associations were estimated using logistic regression. P <=0.05 are in bold. CM = cerebral malaria, SMA = severe malarial anemia, DA = Disc area.

Variable	**Detail**	**Subjects without admission FA**				**Subjects with admission FA**				**Association**		
		Median	IQR	%	number	Median	IQR	%	number	OR	95%CI	p
Number		n/a	n/a	n/a	289	n/a	n/a	n/a	260			
Demographic												
Age	months	39	27-57.5		289	38.5	28-56		260	1	0.99-1.01	0.68
Weight	kg	12.2	10.1-14.95		289	12	10-15		260	0.99	0.96-1.03	0.73
Height	cm	92	84-103		283	92.5	84-104		256	0.99	0.99-1.01	0.87
Sex	male		146	50.52	289		126	48.46	260	1.09	0.78-1.52	0.63
	female		143	49.48			134	51.54				
Clinical												
Duration of fever pre-admission	hours	60	43.5-72		284	60	48-72		247	1	0.99-1.01	0.26
Duration of coma pre-admission	hours	7	4-12		227	9	5-22.75		200	1.01	0.99-1.02	0.12
Rectal temperature	ºC	39	38.05-39.6		289	38.8	38.1-39.57		260	0.97	0.85-1.12	0.7

Variable	Detail	Subjects without admission FA				Subjects with admission FA				Association		
Pulse	Beat/min	160	140-176		289	151	134-171		260	0.99	0.98-0.99	**0.009**
Systolic blood pressure	mmHg	95	87.5-104		277	97	89.25-105.75		244	1.01	0.99-1.02	0.077
Respiratory rate	Breath/min	48	40-56		287	42.5	36-52		260	0.98	0.97-0.99	**0.008**
CSF opening pressure	mmCSF	150	110-190		148	170	116.25-220		134	1	1.00-1.01	**0.046**
Jaundice	negative		228	92.31	247		218	92.37	236	0.99	0.51-1.94	0.98
	positive		19	7.63			18	7.63				
Respiratory distress	negative		178	61.59	289		175	67.31	260	0.78	0.55-1.11	0.16
	positive		111	38.41			85	32.69				
Diagnosis	CM		133	46.02	289		110	42.31	260	1.08	0.91-1.28	0.38
	CM+SMA		156	53.98			150	57.69				
Blantyre Coma score	0		29	10.03	289		18	6.92	260			
	1		122	42.21			120	46.15		1.58	0.84-3.00	0.158
	2		138	47.75			122	46.92		1.42	0.75-2.69	0.276
Hours to reach coma score 3	< 12 hrs		82	34.45	238		27	12.39	218			
	12 to 24 hrs		82	34.45			82	37.61		3.04	1.78-5.17	**<0.001**
	> 24 hrs		74	31.09			109	50		4.47	2.64-7.57	**<0.001**
Clinical outcome	full recovery		225	77.85	289		194	74.62	260			
	sequelae		13	4.5			31	11.92		2.77	1.41-5.43	**0.003**
	death		51	17.65			35	13.46		0.8	0.5-1.27	0.342
	negative		64	22.3	287		47	18.29	257	1.28	0.84-1.95	0.25

Variable	Detail	Subjects without admission FA				Subjects with admission FA				Association		
History of convulsions pre-admission	positive		223	77.7			210	81.71				
Witnessed convulsions on admission	negative		251	87.46	287		222	86.38	257	1.1	0.67-1.81	0.71
	positive		36	12.54			35	13.62				
Witnessed convulsions after admission	negative		192	66.44	289		143	55	260	1.62	1.15-2.29	**0.006**
	positive		97	33.56			117	45				
Investigations												
Peripheral parasitemia	cells	72807.5	15792-301000		280	47720	3295.5-210000		252	0.99	0.99-1.00	0.19
White cell count	cells	9950	6800-15100		274	10000	7200-14400		247	1	0.99-1.00	0.84
Platelet count	platelets	54000	31000-84000		275	59000	31000-103000		245	1	0.99-1.00	0.14
Hematocrit	%	19.9	15.5-24.05		285	19.3	15.3-24.1		257	1.01	0.98-1.03	0.66
Lactate	mmol/L	6.9	3.8-11.6		287	4.85	2.9-9.175		256	0.94	0.90-0.97	**0.001**
HRP2	ng/ml	6765.5	2827-12203		280	7641	3275-10471		259	1	0.99-1.00	0.73
HIV status	negative		223	86.1	259		203	84.94	239	1.1	0.67-1.81	0.71
	positive		36	13.9			36	15.06				
Retinal												

Variable	Detail	Subjects without admission FA				Subjects with admission FA				Association		
Retinal hemorrhages	none		76	28.46	267		60	23.17	259			
	1 to 5		104	38.95			92	35.52		1.12	0.72-1.74	0.612
	6 to 20		53	19.85			52	20.08		1.24	0.75-2.07	0.404
	21 to 50		19	7.12			23	8.88		1.53	0.76-3.07	0.228
	>50		15	5.62			32	12.36		2.7	1.34-5.44	**0.005**
Papilledema	negative		204	76.4	267		175	67.57	259	1.55	1.06-2.28	**0.024**
	positive		63	23.6			84	32.42				
Disc hyperemia	negative		183	69.58	263		177	69.96	253	0.98	0.67-1.43	0.925
	positive		80	30.42			76	30.04				
Macular whitening	none		29	11.07	262		21	8.14	258			
	<1/3DA		159	60.69			97	37.6		0.84	0.46-1.56	0.585
	1/3-1DA		49	18.7			78	30.23		2.2	1.13-4.28	**0.02**
	>1DA		25	9.54			62	24.03		3.42	1.65-7.1	**0.001**
Foveal whitening	none		58	22.22	261		35	13.62	257			
	<1/3 fovea		150	57.47			111	43.19		1.23	0.75-2.0	0.411
	1/3-2/3 fovea		30	11.49			52	20.23		2.87	1.55-5.31	**0.001**
	>2/3 fovea		23	8.81			59	22.96		4.25	2.24-8.05	**<0.001**
Temporal whitening	none		73	28.19	259		35	13.78	254			
	grade 1		140	54.05			101	39.76		1.5	0.93-2.43	0.09
	grade 2		28	10.81			53	20.87		3.95	2.15-7.27	**<0.001**
	grade 3		18	6.95			65	25.59		7.53	3.89-14.56	**<0.001**
Orange vessels	absent		196	77.78	252		122	62.89	194	2.07	1.36-3.13	**0.001**
	present		56	22.22			72	37.11				

Variable	Detail	Subjects without admission FA				Subjects with admission FA				Association		
temporal periphery												
White vessels, temporal periphery	absent		179	71.03	252		148	76.29	194	0.76	0.5-1.17	0.214
	present		73	28.97			46	23.71				
White capillaries, temporal periphery	absent		154	61.11	252		143	73.71	194	0.56	0.37-0.84	**0.005**
	present		98	38.89			51	26.29				

Clinical data from the history, examination, and standard investigations were collected routinely at admission. These included rectal temperature, full blood count (Coulter Counter, Beckman Coulter), and HIV status using two separate tests (Uni-Gold Recombigen HIV-1/2, Trinity Biotech; and Determine HIV-1/2, Inverness Medical). Finger prick blood samples were analyzed to determine parasite species and density, packed-cell volume, blood glucose and blood lactate (Lactate Pro point of care detector (Arkay Inc)). Histidine rich protein 2 (HRP2) was measured retrospectively in stored plasma (Cellabs ELISA).

Supplementary Table 3. Characteristics of included subjects comparing those having admission MRI to those not having admission MRI. Retinal variables are from the worst affected eye. p-values with an * were generated from Kruskal-Wallis test. All other associations were estimated using logistic regression. P <=0.05 are in bold. CM = cerebral malaria, SMA = severe malarial anemia, DA = Disc area.

Variable	**Detail**	**Subjects with FA and MRI**				**Subjects with FA but without MRI**				**Association**		
		Median	IQR	%	number	Median	IQR	%	number	OR	95%CI	p
Number					134				27			
Demographic												
Age	months	43	27-66		134	33	23-54		27	1.01	0.99-1.03	0.22
Weight	kg	11.9	10-15		134	11	9-15		27	1.03	0.94-1.14	0.51
Height	cm	93.0	81-106		132	93	81-104		26	1.01	0.98-1.04	0.49
Sex	male			51.5	134			44.4	27	0.75	0.33-1.73	0.51
	female			48.5				55.6				
Clinical												
Duration of fever pre-admission	hours	64	48-72		128	48	42-72		26	1.00	0.99-1.02	0.52
Duration of coma pre-admission	hours	9	5-21		105	9	5-18		21	1.01	0.98-1.04	0.57

Rectal temperature	ºC	38.9	38.1-39.7		134	38.8	38.1-39.4		27	1.06	0.74-1.52	0.74
Pulse	Beat/min	149	132-169		134	152	130-171		27	1.00	0.98-1.02	0.97
Systolic blood pressure	mmHg	96	89-104		120	95	86-101		26	1.02	0.99-1.06	0.23
Respiratory rate	Breath/min	41	36-52		134	48	38-56		27	0.99	0.95-1.02	0.44
CSF opening pressure	mmCSF	170	130-232		62	185	122-217		16	1.00	0.99-1.01	0.92
Jaundice	negative			96.3	134			92.6	27	0.48	0.09-2.64	0.4
	positive			3.7				7.4				
Respiratory distress	negative			72.4	134			66.6	27	0.76	0.31-1.85	0.55
	positive			27.6				33.3				
Diagnosis	CM			42.5	134			51.8	27	1.21	0.8-1.83	0.37
	CM+SMA			57.5				48.2				
Coma score	0			6.7	134			7.4	27			
	1			51.5				33.3		1.7	0.32-9.16	0.53
	2			41.8				59.3		0.78	0.15-3.97	0.76
Time to reach coma score 3	hours	28	18-52		109	16	10-28		23	1.01	0.99-1.02	**0.006***

Clinical outcome	full recovery			73.9	134			77.8	27			
	sequelae			11.9				3.7		3.39	0.43-27.0	0.25
	death			14.2				18.5		0.81	0.27-2.40	0.69
Witnessed convulsions on admission	negative			17.9	134			19.2	26			
	positive			82.1				80.8		1.09	0.37-3.18	0.87
Witnessed convulsions after admission	negative			85.5	131			92.6	27			
	positive			14.5				7.4		2.12	0.46-9.70	0.33
Investigations												
Peripheral parasitemia	cells	39360	1270-176000		129	50550	19200-182000		26	1.00	1.00-1.00	0.436
White cell count	cells	10200	6500-14850		125	9500	7650-12950		26	1.00	1.00-1.00	0.63
Platelet count	platelets	58000	30000-97000		123	47500	25750-86750		26	1.00	1.00-1.00	0.68
Hematocrit	%	20	17-25.1		131	18.7	15.6-23.2		27	1.05	0.98-1.12	0.18
Lactate	mmol/L	4.6	2.8-8.95		134	4.6	3.0-11.3		23	0.96	0.87-1.06	0.45

HRP2	ng/ml	8415	4133-13690.8		134	9470	2790-11070		27	1.00	1.00-1.00	0.92
HIV status	negative			84.3	127			88.5	26			
	positive			15.8				11.5		1.43	0.39-5.23	0.59
Retinal												
Retinal hemorrhages	none			27.1	133			29.6	27			
	1 to 5			36.8				29.6		1.36	0.47-3.97	0.57
	6 to 20			18.1				18.5		1.07	0.31-3.65	0.92
	21 to 50			6.8				7.4		1.00	0.18-5.55	1.00
	>50			11.3				14.8		0.83	0.22-3.19	0.79
Papilledema	negative			72.9	133			62.9	27			
	positive			27.1				37.0		0.63	0.26-1.5	0.29
Disc hyperemia	negative			70	130			84.6	26			
	positive			30				15.4		2.4	0.76-7.29	0.14
Macular whitening	none			9.9	132			3.7	27			
	<1/3DA			30.3				44.4		0.26	0.03-2.17	0.21
	1/3-1DA			32.6				18.5		0.66	0.07-6.18	0.72
	>1DA			27.3				33.3		0.31	0.04-2.67	0.29
Foveal whitening	none			15.9	132			15.4	26			
	<1/3 fovea			38.6				46.2		0.81	0.23-2.8	0.74
	1/3-2/3 fovea			16.7				19.2		0.84	0.2-3.5	0.81
	>2/3 fovea			28.8				19.2		1.45	0.35-5.9	0.61

Orange vessels, temp periphery	absent			62.9	108			75	20			
	present			37.0				25		1.76	0.6-5.22	0.31
White vessels, temp periphery	absent			86.1	108			75	20			
	present			13.9				25		0.48	0.15-1.53	0.22
White capillaries, temp periphery	absent			85.2	108			75	20			
	present			14.8				25		0.52	0.17-1.64	0.27
Macular capillary non-perfusion	Grade 0 or 1			6.87	131			11.54	26			
	Grade 2			47.33				50.00		1.59	0.38-6.69	0.53
	Grade 3 or 4			45.80				38.46		2.00	0.46-8.68	0.36
Peripheral CNP	Grade 0 or 1			39.85	133			25.93	27			
	Grade 2			24.81				25.93		0.62	0.2-1.94	0.41
	Grade 3 or 4			35.34				48.15		0.48	0.18-1.30	0.15
Punctate focal leak	None			63.43	134			66.67	27			
	1-5 sites			28.36				33.33		0.89	0.37-2.17	0.81
	>5 sites			8.21				0.00		-	-	-
Large focal leak	None			83.58	134			77.78	27			
	1 site			6.72				0.00		-	-	-
	>1 site			9.70				22.22		0.41	0.14-1.19	0.10

Large/small venule leak	None			56.39	133			46.15	26			
	Grade 1			32.33				26.92		0.98	0.36-2.68	0.97
	Grade 2 or 3			11.28				26.92		0.34	0.12-1.01	0.053
Post-capillary venule leak	None or grade 1			75.19	133			53.85	26			
	Grade 2			17.29				26.92		0.46	0.17-1.27	0.13
	Grade 3 or 4			7.52				19.23		0.28	0.08-0.94	**0.04**
Disc leak	Absent			18.66	134			0.00	27			
	Present			81.34				100.00		-	-	-
Intravascular filling defect in large arterioles	Absent			86.15	130			77.27	22			
	Present			13.85				22.73		0.55	0.18-1.67	0.29

530

Supplementary Table 4. Mediation analysis of causal routes from large focal leak (LFL) to death.

This assumes that LFL is proportionate manifestation of analogous leakage in the brain. One path involves two steps: LFL to severe brain swelling, and severe brain swelling to death; the effect of LFL on death is mediated by severe brain swelling. The other goes directly from LFL to death; LFL (or more precisely, the intracranial analogue represented by LFL) causes death directly. The absence of other connectors between boxes illustrates the assumption that there are no unmeasured exposure-mediator, exposure-outcome, or mediator-outcome confounders. The natural indirect effect describes the effect of the exposure (LFL) on the outcome (death) that operates through the mediator (severe brain swelling). In comparison the natural direct effect represents whatever effect would remain after disabling the path between the exposure and the mediator.

	Estimate	Standard error	P	95% CI	n
Controlled direct effect	1.60	0.65	0.47	0.45 to 5.66	133
Natural direct effect	1.60	0.65	0.47	0.45 to 5.66	133
Natural indirect effect	2.04	0.30	**0.02**	1.14 to 3.66	133
Marginal total effect	3.26	0.67	0.08	0.87 to 12.22	133